Inorganic Chemistry

Article

pubs.acs.org/IC

Inorganic Polar Blocks into Controlled Acentric Assemblies

D. Endara,[†] M. Colmont,[†] M. Huvé,[†] F. Capet,[†] J. Lejay,[‡] P. Aschehoug,[‡] and O. Mentré*,[†]

[†]UCCS, UMR 8181, Université lille Nord de France, USTL, F-59655 Villeneuve d'Ascq, France

[‡]LCMCP-UMR 7574 ENSCP, 11 rue Curie, F-75231 Paris Cedex 05, France

Supporting Information

ABSTRACT: We show here a strategy to predict the crystal structure, formulate, and prepare new noncentrosymmetric (NCS) bismuth−phosphate based compounds. It is based on the cooperative-arrangement of polar building units (BUs) which can be created at particular stoichiometric conditions. The arrangement of such BUs into NCS compounds arise from the shortest-periodicity of repartition of the cationic charges in NCS structures than in the plausible, but never observed centrosymmetric polytypes. This work validates the possibilities for the prediction of an extended series of novel compounds, tuning the size of BUs within a variety of controlled edifices. Despite their closed chemical composition, all the predicted terms appeared strikingly stable at precise stoichiometries.

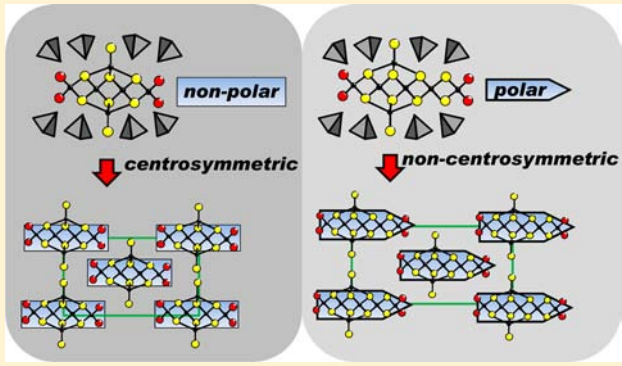

INTRODUCTION

The search for new second-order nonlinear optical (NLO) materials is of high interest due to their applications in photonic and laser technologies.[1] The structural conditions for such materials correspond to those for piezoelectricity, which means crystallizing in 20 of the 21 noncentrosymmetric (NCS) point groups, at the exception of the 432 crystal class.[2] Then, NCS compounds exhibit second-harmonic generacy (SHG) with various efficiency depending on their second-order electric polarizability. This latter is mainly driven by the resulting dipolar momentum summed inside one unit cell. Here, we are interested by the striking possibility to produce novel NCS materials using a rational predictive approach in a favorable chemical system.

Among others, two conditions are well-recognized to favor NCS or polar compounds: (i) the contribution of cations with stereochemically active lone pair electrons such as Sn^{2+}, Pb^{2+}, Sb^{3+}, Bi^{3+}, Se^{4+}, Te^{4+}, etc.; (ii) second-order Jahn−Teller d^0 transition metals (Ti^{4+}, Nb^{5+}, W^{6+}, etc.), both of those cationic types being susceptible of strongly distorted acentric anionic local coordination.[3] However, these conditions are not sufficient by themselves since only a cooperative arrangement of local polarities could conserve the NCS character of the crystal structure. It follows that the rational conception of NCS compounds remains a rare science and that the discovery of most of the recent strongly efficient NLO materials is often fortuitous. On the opposite, examples of fully rationalized so-called "design" approaches are noteworthy. For instance the recent Aurivilius-like $BiO(IO_3)$ compound shows an expected NCS arrangement of polar iodates groups.[4] Another example concerns the $ACuTe_2O_7$ (A = Sr^{2+}, Ba^{2}+, or Pb^{2+}) for which the effect of the influence of the A nature on the polarizability has been fully explained on the basis of valence concepts. For perfect alignment of the polar subunits (A = Ba^{2+} case), a macroscopically polar material is formed.[5] Other developed approaches in the field of organometallic compounds deal with the use and comprehension of polar MO_xF_y building groups (M = Nb^{5+}, W^{6+}, for instance) as ligands of transition metals. In some cases, the final edifice corresponds to NCS structure due to the alignment of the polar bricks, e.g. $Cd(3\text{-apy})_4NbOF_5$.[6] Similar strategically rationalized elaborations of "pure-inorganic" materials are indeed less common, since the identification and the controlled arrangements of more complex building units, including polar ones, are mediated by a number of parameters such as the chemical composition, the temperature, the pressure. It is generally restricted to the class of 2D-layered compounds in which modular building units (BUs) stack with respect to charge compensation and interfacial coherence.[7] Here, in Bismuth oxo phosphates, we investigated the identification of complex inorganic polar building units and predicted their controlled arrangements into a series of new polar compounds.

EXPERIMENTAL SECTION

Synthesis. Powders were synthesized by solid-state reaction between Bi_2O_3, CuO/ZnO, Li_2CO_3, and $(NH_4)_2HPO_4$ precursors. Several heating/grinding stages from 150−800 °C are applied, and finally, the samples are kept at 800 °C for 70 h in alumina crucibles. Finally, the samples are quenched to room temperature. Single crystals were obtained by melting the concerned polycrystalline samples at 950 °C and controlled cooling (2 °C/h) to room temperature. Generally crystals grow in a homogeneous mixture, but we systematically found

Received: July 3, 2012
Published: August 21, 2012

   dx.doi.org/10.1021/ic3014305 | *Inorg. Chem.* 2012, 51, 9557−9562

after melting a polycrystalline sample with a given targeted crystal structure, a large part of single crystals that conserve the parent-form.

Powder XRD. Powder patterns were collected at room temperature using a D8 Advance Bruker AXS diffactometer, Cu Kα radiation with steps of 0.02°.

Single Crystal X-ray Diffraction (XRD). Single crystal XRD data were collected using a Bruker X8 APPEX II diffractometer (λ = 0.71073 Å). Intensities have been extracted from the collected frames using the program Saint Plus 6.025.[17] The lattice parameters were defined from the complete data set. Absorption corrections were performed for both studied crystals using the multiscan SADABS[18] program. The structural refinements have been performed with Jana 2006.[19]

RESULTS AND DISCUSSION

Transmission Electron Microscopy (TEM). Electron diffraction patterns (EDP) and images were obtained on a FEI technai G220 transmission electron microscope equipped with a precession system. The material was crushed and dispersed on a holey carbon film deposited on a Cu grid.

Second Harmonic Generation. SHG efficiency, was measured using a pulsed YAG:Nd^{3+} laser (1064 nm with 10 Hz frequency, 8 ns pulse duration) on a thin powder layer. This thickness and the incident beam diameter being largely bigger than the particle size, we ensure that a large number of particles with random orientation were stroked. The incident beam is cutoff with several filters, and SHG is collected by using a Pacific photomultiplier (PMT), visualized, and time-averaged on a Tektronix oscilloscope. However according to the small quantity of available amount single-phase powder, it was not to work with homogeneous particle size, and the results should be considered as semiquantitative only.

Structural Context. We are interested in the organization of bismuth-based 1D sizable building units (BUs) into new $X^{V}O_4$ containing frameworks (X = P, As, V). In the Bi_2O_3–X_2O_5–MOx (M = various cations) ternary diagrams, structural filiations between most of the phases in competition can be generalized with respect to systematically found sizable BUs.[8] For the first time we present here an unified empirical model which allows a general vision of all crystal structures of these systems and an easy distinction of the BUs and their relative arrangement. In our experience, in the concerned chemical systems, a majority of reported compounds can be structurally deduced from the X/M for Bi cationic substitution for Bi in the δ-Bi_2O_3 fluorite like crystal structure. Indeed, in its ideal form, the high temperature δ-Bi_2O_3 is well described by a regular three-dimensional (3D) lattice of edge-sharing (O,□)Bi_4 oxo-centered tetrahedra,[9] Figure 1a. The filiation of X/M-doped compounds with the parent fluorite structure can be easily verified by the conservation of at least one lattice parameter (conventionally the *b*-axis) of ∼5.4 Å (or any supercell-related value) that represents the height of two edge-sharing OBi_4. It follows that after projection along the *b*-axis, the cations are aligned along a regular grid-network with two possible *out-of-plane* coordinates: *y* and $y + {}^1/_2$. From a careful look at several reported structural types in these chemical systems, we have observed that the XO_4 tetrahedra substitute the Bi-sites with important constraints, such that the cationic grid persists but is strongly distorted. The degree of distortion is proportional to the amount of incorporated XO_4 groups. Strikingly, for X = P and As, the number of consecutive XO_4 along all grid-lines never exceeds two, creating sizable infinite 1D-ribbons, *n*-$O(Bi)_4$ tetrahedra wide, surrounded by rows of Bi and XO_4 groups. The BUs mentioned above correspond to the created

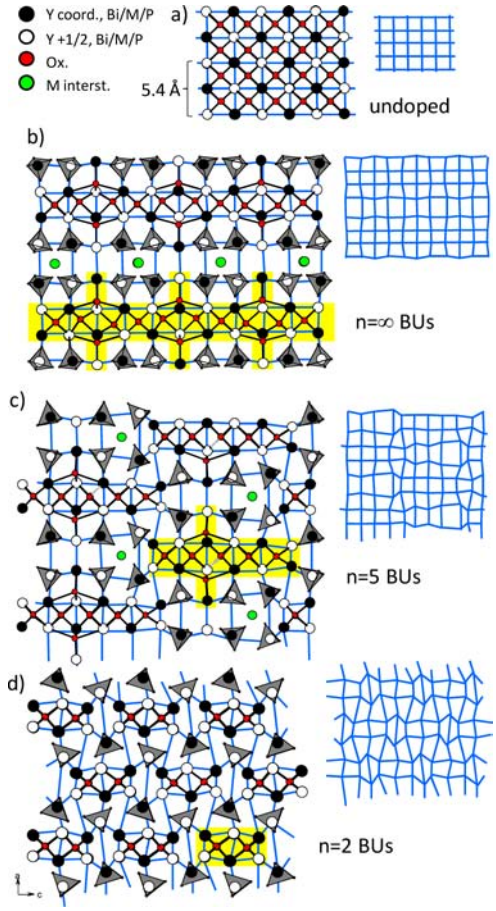

Figure 1. Crystal structure projected along the ∼5.5 Å long axis (= *b* by convention) and the corresponding cationic grid-lattice in blue, for an ideal fluorite like Bi_2O_3 (a) infinite ribbonlike BUs in $BiM_2O_4(PO_4)_2$, (b) *n* = 5 tetrahedra long BUs in $Bi_{13.67}Cu_{2.33}Li_2O_{12}(PO_4)_6$, (c) and *n* = 2 tetrahedra long BUs in $BiM_2O_2(PO_4)$. (d) Individual BUs are shown in yellow and include edge (Bi/M), core (Bi), and excrescence (Bi) type cations.

1D-ribbons and their neighboring Bi excrescences and appear surrounded by XO_4 groups. The Bi^{3+} lonepair is stereoactive in these systems and point externally to the ribbons (Supporting Information section S0), responsible for the good anionic mobility in the BIMEVOX series with related infinite $[Bi_2O_2]^{2+}$ layers.[10] In the compounds of the Bi_2O_3–X_2O_5–MOx systems, M is most often disordered at the edges of ribbons into mixed Bi/M sites. Also, we find interstitial M atoms in the channels created between four adjacent XO_4 walls which do not participate to cationic grid-sublattice. Figure 1b, c, and d shows the progressive distortion of the cationic lattice from 2D-infinite ribbons in $Bi_4MO_4(PO_4)_2$,[11] to *n* = 5 and 2 tetrahedra long ribbons.[12−14] On these figures, the ribbons are evidenced by yellow areas while interstitial M cations of the tunnels are shown in green. On the basis of such an extended rational model with sizable ribbon length, the structural prediction, formulation, and elaboration of novel archetypes have been successfully achieved for several terms through the setting of unified compositional compound that remain available for any *n* ribbon-size present in reported and hypothetical compounds.[11,15] Furthermore, variously sized BUs can also coexist in the materials leading to the unlimited potentiality for novel original members. Currently, the evidence of variously sized BUs that extend from *n* = 1 to ∞[11] in a number of related

dx.doi.org/10.1021/ic3014305 | Inorg. Chem. 2012, 51, 9557−9562

compounds emphasizes the striking thermodynamic stability of polymorphs in competition, despite very closed chemical compositions.

Prediction of New Terms. As briefly described above, in the concerned series of materials, the arrangement between polycationic BUs, PO_4, and interstitial channels can be fully rationalized, at least in the cases dealing with intergrowths between one single-nature of BUs. This means that, according to systematic rules, the choice of the n values leads to a defined structural model assorted with a typical chemical formula $Bi_aM_b(PO_4)_cO_d$.[11] In detail Bi_a includes Bi^{3+} in the cores of BUs (= Bi^{core}: 100% Bi sites), at their edges (=Bi^{edge}: mixed Bi/M sites), and the surrounding ones (= Bi^{Ex}, for excrescence). M_b include interstitial M cations (= M^{tunnel}) and mixed Bi/M sites (= M^{edge}). Finally, the O_d stoichiometry concerns oxygen atoms inside the ribbons and includes both the $O(Bi/M)_4$ tetrahedra and those of the $(O-Bi^{Ex})$ excrescences, one per Bi^{Ex}. For charge electroneutrality, the potentiality of aliovalent $(Bi^{3+}/M^{n+})^{edge}$ sites and aliovalent interstitiitial M^{tunnel} cations (e.g., Zn^{2+}/Li^+) allows for chemical degrees of freedom to stabilize the targeted edifice. We have intensively studied systematic relationships between structures and chemical formulas and found systematic formulation rules as a function of the ribbon width n. We have established that long-sized ribbon BUs ($n_{tetrahedra} > 3$)[11,15] have the general formula $\{(M/Bi)^{Edge}{}_4Bi^{Core}{}_{2n-2}Bi^{Ex}{}_{2Int[(n-1)/3]}O_{2n+2Int[(n-1)/3]}\}^{x+}$ surrounded by $2((n-1) - Int[(n-1)/3])PO_4$ per ribbon. $Int[x]$ denotes the integer part of x. For the determination of the number of created interstitial tunnels, two cases should be distinguished depending on the n-size.

(i) $n \neq 3n'$: there are $Int[(n+1)/3] - 1$ tunnels per ribbon, which leads to the compounds formulated $\{ribbon\}_1(PO_4)_{2((n-1)-Int[(n-1)/3])}M^{tunnel}{}_{\sim 2\{Int[(n+1)/3]-1\}}$. We have ~2 M cations per tunnel in a formula unit.

(ii) $n = 3n'$: there are $n/3$ tunnels per ribbon, which leads to the compounds formulated $\{ribbon\}_1(PO_4)_{2((n-1)-Int[(n-1)/3])}M^{tunnel}{}_{\sim 2n/3}$.

Polar Bus into Acentric Intergrowths. As shown in the Figure 1c, the $n = 5$ tetrahedra-long BUs are polar with respect to the presence of decorating Bi centers that divide the ribbons in two unequal parts, i.e. $n = 2$ and $n = 3$ segments. Strikingly, according to the maximal presence of two PO_4 along the cationic grid-lines mentioned above, a similar polar character is expected for all ribbons with $n = 3n' + 2$, e.g. $n = 5$, 8, 11, ..., etc. This peculiar feature is depicted in the Figure 2.

Among the "potential" compounds formed of polar BUs, the $n = 5$ case has been the first reported compound with polar BUs[12] arranged into a NCS crystal structure. A compound with the expected crystal structure has been fortuitously prepared during the "blind" investigation of the $Bi_2O_3-CdO-CuO-P_2O_5$ quaternary diagram, and its NCS crystal structure was deduced by means of high resolution electron microscopy and refined using XRD powder Rietveld refinement of the $Bi_{10}Cd_4Cu_2(PO_4)_6O_{12}$ sample (nearly single-phase material with $n = 5$ ribbons). Note that oxygen of the phosphate groups have not been located due to the strong PO_4 configurational disorder which results from the neighboring mixed cationic sites. At least, this incomplete model validates the *head-to-tail* arrangement of polar $n = 5$ tetrahedra long BUs into a NCS symmetry (space group *Ibm*2).

The compound corresponding to $n = 11$ was voluntarily prepared[15] after it was observed by HREM as an extended

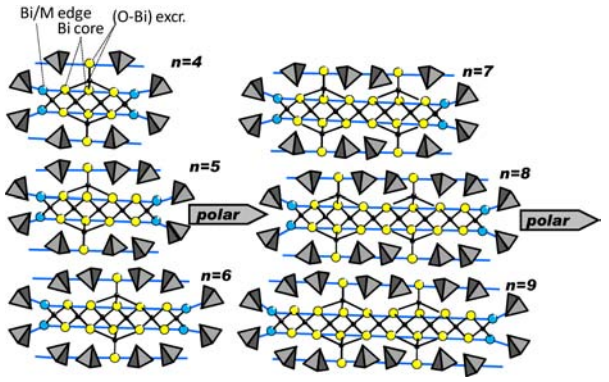

Figure 2. Ideal ribbonlike BUs of general formula $\{(M/Bi)^{Edge}{}_4Bi^{Core}{}_{2n-2}Bi^{Ex}{}_{2Int[(n-1)/3]}O_{2n+2Int[(n-1)/3]}\}^{x+}$ and their PO_4 surrounding. The surrounding by (OBi) excressences and (PO_4) involve polar BUs for $n = 3n'+2$.

defect in a sample of the $Bi_2O_3-ZnO-LiO-P_2O_5$ ternary system. After several syntheses to isolate the single-phase material, the sample of formula $Bi_{28.64}Zn_{3.99}Li_{4.1}(PO_4)_{14}O_{28}$ led to a single phase material. Its crystal structure from single crystal XRD (obtained after melting/slow-cooling of the powder) also show a *head-to-tail* arrangement of BUs in the NCS *Im* space group. In this paper, we have focused on the extended rationalization (prediction−formulation−synthesis−characterization) of $n = 5$ and 8 in order to validate the prediction and conception of acentric compounds. In a first stage it seems of fundamental importance to analyze the reasons for cooperative arrangement of the BUs into NCS materials rather than the *head-to-head* arrangement (centrosymmetric) in the $n = 3n'+2$ cases met previously. These two antagonist models are shown in Figure 3 for hypothetical materials with $n = 8$ tetrahedra-long BUs. They would ideally crystallize in the *Bbm*2 (*head-to-tail*) and *Pbma* (*head-to-head*), respectively. Both compounds are plausible in terms of

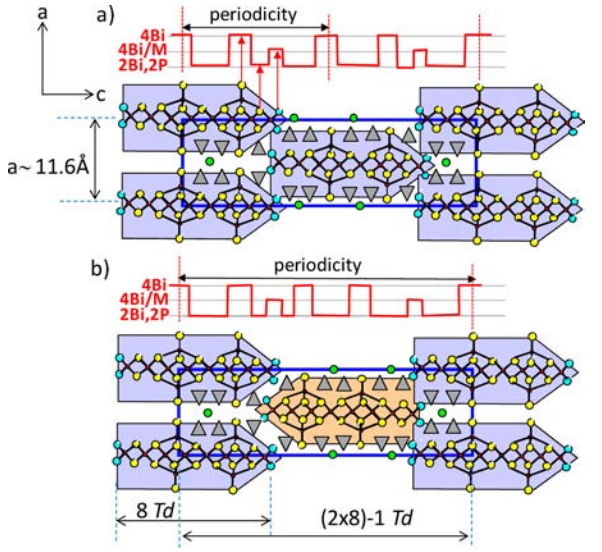

Figure 3. Ideal projection along the b parameters of hypothetical crystal structures with $n = 8$ tetrahedra long polar BUs (orthorhombic unit cell, $a \sim 11.6$, $b \sim 5.4$, $c \sim 41.5$ Å). The *head-to-tail*-arrangement between BUs ideally crystallizes in the *Bbm*2 space group (a), the antiferro-arrangement ideally crystallizes in the *Pbma* space group (b). The cationic lattice density projected along b is shown by the red plot.

dx.doi.org/10.1021/ic3014305 | *Inorg. Chem.* 2012, 51, 9557−9562

interatomic separations and would ideally conserve the same unit-cell volume. Analyzing these two hypothetical models, it turns out that the projection along the vertical grid-lines (*a*-axis) of the cationic content per unit-cell leads to three different states along the *c*-axis: (i) **4 Bi** (cores and excressences), (ii) **4 Bi/M** mixed sites (edges of ribbons), (iii) **2 Bi** (cores) + **2 P** atoms. A qualitatively projected "electronic density" is shown in the Figure 3 and follows a shortest periodicity (= $c/2$) in the NCS case compared to c in the centrosymmetric case. Intuitively, the shortest periodicity is expected to bring a greater thermodynamical stability to the structure, i.e. in the polar crystal structure. At this stage of our work, this empirical argument is proposed as the driving force for the systematic predominance of the NCS enantiomers already observed for compounds with n = 5 and 11 BUs.[12,15]

Elaboration of Novel Acentric Materials. For each given n value, from the prior investigations of related compounds, an ideal crystal structure can be partially elaborated. The ideal symmetry is systematically orthorhombic with unit cell parameters $a \sim 11.6$, $b \sim 5.4$, $c \sim (2n - 1) \times 2.8$ Å. Here, the value of the *c*-parameter counts the number of $O(Bi,M)_4$ tetrahedra (~2.8 Å thick) present along *c*, taking into account the overlap between two superposed ribbons along the *a*-axis; see Figure 3b. The coordinates of every cations and oxygen of the BUs can be found from the fluorite-heritage described above; see Figure 1. The resulting idealized structural model allows for the calculation of an ideal XRD powder pattern using an ideal space group easily found from the analysis of the symmetry between adjacent BUs in the unit-cell (Supporting Information section S1).

For n = 5, the predicted general formula leads to $\{(M/Bi)^{Edge}{}_4Bi^{Core}{}_8Bi^{Ex}{}_2O_{12}\}(PO_4)_6M^{tunnel}{}_{\sim 2}$. The expected ferro-lattice (NCS) characteristics are $a \sim 11.6$, $b \sim 5.4$, $c \sim 25.1$ Å, *Ibm*2 space group. To prepare such compounds, we have screened the pertinent area of the Bi_2O_3–CuO–ZnO–Li_2O–P_2O_5 phase diagram tuning the (M/Bi) ratio and the tunnel content (Supporting Information section S2). The $[Bi_{12}Cu_2O_{12}](PO_4)_6Li_2$ composition leads to a single-phase material (orthorhombic I, a = 11.4352(1), b = 5.4225(7), c = 25.0365(3) Å) from the systematic comparison of experimental XRD patterns with the theoretical XRD pattern calculated for an ideal n = 5 NCS-arrangement, Figure 4a. Single crystals have been isolated after melting the polycrystalline powder.

For n = 8, the characteristics of the expected NCS-phase are $a \sim 11.6$, $b \sim 5.4$, $c \sim 42$ Å, space group *Bbm*2. The predicted formula is $\{(M/Bi)^{Edge}{}_4Bi^{Core}{}_{14}Bi^{Ex}{}_4O_{20}\}(PO_4)_{10}M^{tunnel}{}_{\sim 4}$. Using the same process in the Bi_2O_3–ZnO–P_2O_5 and Bi_2O_3–ZnO/CuO–Li_2O–P_2O_5 diagrams, two samples showing the expected single-phase XRD pattern have been identified (Supporting Information section S2), with stoichiometries $[Bi_{20}Zn_2O_{20}][PO_4]_{10}Zn_{1.34}Li_{3.33}$ (orthorhombic B-centered, a = 11.5915(4), b = 5.4392(2), c = 41.8520(2) Å) and $[Bi_{21.2}Zn_{0.8}O_{20}](PO_4)_{10}Zn_{4.7}(O)_{2.3}$ (orthorhombic B-centered a = 11.6132(7), b = 5.3904(5), c = 42.1938(7) Å). We note in the latter that the single phase material was obtained with an excess of oxygen denoted $(O)_{2.3}$ in regard to the allowed oxygen stoichiometry. For both, it is probable that the real cationic repartition in tunnels and edges of BUs do not fully respect the stoichiometry used in the synthesis. The Figure 4b shows the good matching between the expected and experimental XRD patterns. Single crystals of the n = 8 compound have been prepared after heating at 950 °C and slow cooling until 700 °C (sweep = 3.5 °C/h) of the powder

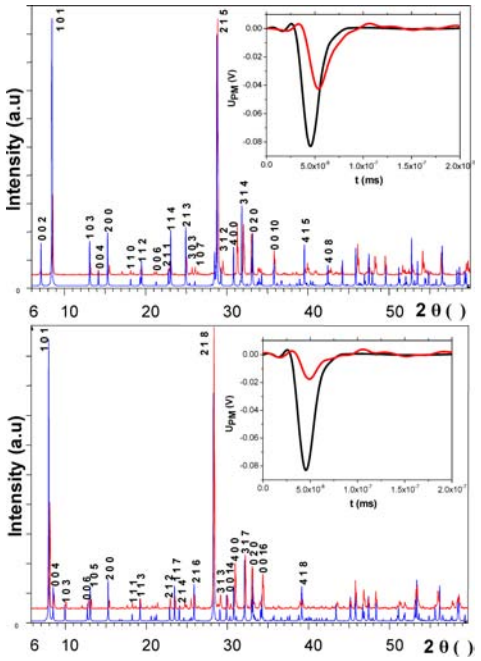

Figure 4. Predicted and experimental XRD powder pattern for (a) $[Bi_{12}Cu_2O_{12}](PO_4)_6Li_2$, i.e. NCS structure with n = 5 BUs. (b) $[Bi_{20}Zn_2O_{20}][PO_4]_{10}Zn_{1.34}Li_{3.33}$, i.e. NCS structure with n = 8 BUs. The insets show the green emittted signal (red) compared to KDP (black).

corresponding to the $Bi_{18}Zn_8O_{20}(PO_4)_{10}$, but a large concentration of intergrowth-defects were detected. Finally single crystal suitable for XRD analysis were obtained from the same treatment applied to $Bi_{20.6}Cu_{2.6}Li_3O_{20}(PO_4)_{10}$.

Crystal Structure Certification. Details of the single crystal structure determination and refinements for the n = 5 and 8 new compounds are given in the Supporting Information section S3. Typically for both compounds, metal atoms are located using direct-methods[16] while anions were found on subsequent Fourier-difference maps. The space group corresponds to the ideal one (*Bbm*2) for n = 8, while for n = 5, due to supercell spots, the crystal structure was refined in the $Pbn2_1$ subgroup of the ideal *Ibm*2, but the model remains essentially as predicted. As commonly observed cationic sites at the edges of ribbon contain mixed Bi/Cu cations. An average position was refined. However, due to Bi^{3+} vs Cd^{2+} different ionic radii, severe local shifts of the coordinated oxygen atoms are expected. Indeed, as systematically observed in related compounds,[8,12,15,16] this results in multiple orientations of the PO_4 groups bordering these sites, among which only the predominant orientations have been located. Finally, the tunnels appear fully occupied by Li^+ cations for n = 5 (one single site) but disordered over two mixed Cu/Li sites for n = 8. At this level also local differences of coordinations are expected along the tunnel axis but were not examined in the scope of this paper, due to the consideration of a single PO_4 orientation per Phosphorus site forming the channel-walls. Both crystal structures respect the predicted NCS character due to the *head-to-tail* arrangement of polar BUs. For n = 5, the structure was already given by anticipation in Figure 1c, while for the n = 8 case, it corresponds to Figure 3a. Pertinent crystallographic data and refinement parameters are gathered in Table 1, for the three available single-crystal NCS structure refinements performed so far with polar BUs, n = 5, 8 (this work), and 11.[15]

dx.doi.org/10.1021/ic3014305 | *Inorg. Chem.* 2012, 51, 9557–9562

Table 1. Crystallographic Data and Reliability Factors for Polar Compounds from $n = 3n' + 2$ Tetrahedra Long Polar BUs

BU size = n tetrahedra	lattice parameter (Å, deg)	space group	R_1, wR_2 %($I > 3\sigma(I)$)
	$[Bi_{11.67}Cu_{2.32}O_{12}]_{ribbon}[Li_2]_{in\ 1\ tunnel}[PO_4]_6$		
$n = 5$	$a = 11.4096(4)$	$Pbn2_1$ (no. 33)	4.59, 4.88
	$b = 5.4333(2)$		
	$c = 25.1315(9)$		
	$[Bi_{19.80}Cu_{2.19}O_{20}]_{ribbon}[Cu_{0.64}Li_{3.36}]_{in\ 2\ tunnels}[PO_4]_{10}$		
$n = 8$	$a = 11.5048(10)$	$Bbm2$ (no. 40)	4.87, 6.04
	$b = 5.4565(6)$		
	$c = 41.656(3)$		
	$[Bi_{28.64}Zn_{1.36}O_{28}]_{ribbon}[Zn_{2.64}Li_{4.10}]_{in\ 3\ tunnels}[PO_4]_{14}$		
$n = 11$	$a = 11.579(3)$	Im (no. 8)	8.17, 7.74
	$b = 5.476(1)$		
	$c = 59.0149(14)$		
	$\beta = 90.28(2)$		

Due to the difficulties to increase the grain size of the $n = 5$ and 8 polycrystalline samples while preserving single phase materials and the difficulty to prepare a large amount of our compounds, only semiquantitative second-harmonic-generacy (SHG) tests have been performed, with the aim to validate the NCS character. Results are shown in the insets of the Figure 4 by comparison to KDP performances in approximately the same amount, but unfortunately with different microstructure. Both compounds are SHG active, but the green emission (λ = 532 nm) is significantly weaker than KDP. Besides the inhomogeneous distribution of small grains, such weak signals (SHG being mainly driven by the electric polarization[2]) could reasonably be explained by the following: (i) The disordered character of our phases (tunnels occupancy, edges of BUs, etc.). (ii) The net dipolar moment which after summing individual polyhedral contributions is expected low. Indeed, predominant bricks of the polar BUs are OBi_4 tetrahedra with weak local dipolar moments. In fact, the major contributions concern the strongly acentric OBi_5 excrescences with orientations that almost cancel each other in the $n = 8$ ribbons (weaker SHG) but interplay cooperatively for $n = 5$ (stronger SHG), Figure 5, in good agreement with the experimental relative efficiency between both compounds. (iii) Also, it turns out that under the intense laser beam, our samples darkened as already mentioned for the $n = 11$ compound.[15] The analysis of this phenomenon is under progress. At least, in the scope of this article, we qualitatively validated the elaboration of predicted NCS materials.

Multiple Intergrowths. We have already mentioned the striking ability of these chemical systems to display a variety of intergrowths between different ribbons, while regular extended structures can be achieved at particular stoichiometries. For instance, for the crystals ($n = 8$) with a high concentration of defects mentioned above, the [010] zone axis patterns and lattice images show the alternation of various n-sized BUs accordingly to multiple local c-periodicities, Figure 6a–e. The selected area shown in Figure 6f displays alternation of $n = 5$ to 11 tetrahedra-wide BUs.

CONCLUDING REMARKS

Besides the general interest for the prediction of novel "tailor-made" inorganic compounds, we have shown here the possibility to design noncentrosymmetric materials using a Lego-like assembly of complex Bi^{3+} based polar building units. Their preferred arrangement into NCS crystal structures seems favored by electric charge repartition in the crystal. The successful stabilization of three predicted NCS polytypes with sizable BUs is a source of inspiration and opens the route to an extended series of novel compounds. In spite of the possible attribution of a general chemical formula for all predicted compounds, the accurate composition and precise synthesis conditions remain limiting factors, to achieve targeted compounds as single-phase materials. Finally in all these compounds, the cationic lattice being related to the ideal fluorite-like cationic lattice (δ-Bi_2O_3) with P and M replacing Bi, it is noteworthy that we propose for the first time an unified model that enable an overview of direct structural relationships in these series.

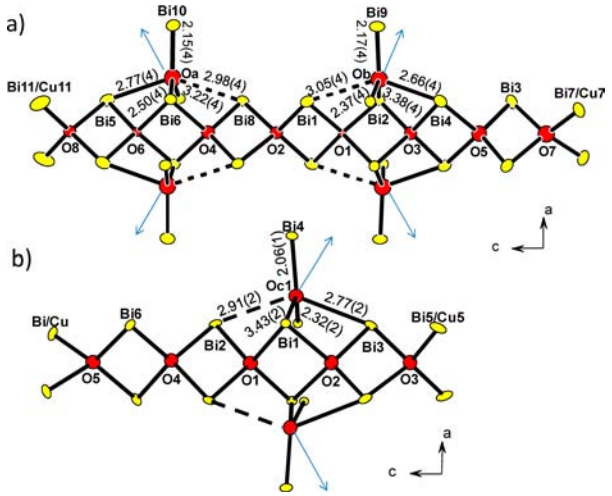

Figure 5. Dipolar charge along (a) the $n = 8$ tetrahedral long polar BUs for $[Bi_{20}Zn_2O_{20}][Zn_{1.34}Li_{3.33}][PO_4]_{10}$ (The dipoles of central OBi_4 and $O(Bi,Cu)_4$ are expected weak while those of OBi_5 are strong but should partially cancel each other.) (b) the $n = 5$ tetrahedral long polar BUs in $[Bi_{12}Cu_2O_{12}][Li]_2[PO_4]_6$. Strong moments are expected for OBi_5 and are arranged in a cooperative manner from one ribbon to the other ones.

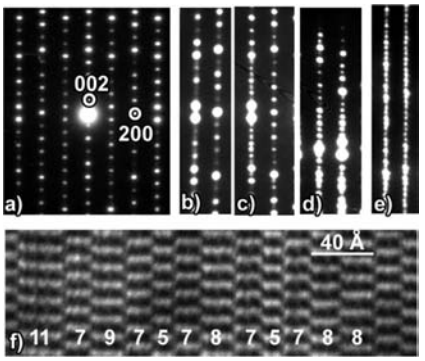

Figure 6. [010] ZAP of different area of the same crystal enhancing (a) a well-ordered area of with $n = 8$ BUs and (b–e) the same $n = 8$ c-parameter with extra streaks or spots. (f) HREM image for ZAP image e displaying several disordred BUs.

ASSOCIATED CONTENT

Supporting Information

Lonepair effect in the related series of compounds; ideal structural model for noncentrosymmetric compounds; syn-

dx.doi.org/10.1021/ic3014305 | Inorg. Chem. 2012, 51, 9557–9562

thesis of the expected acentric compounds; single crystal structure refinement for n = 5 and 8. This material is available free of charge via the Internet at http://pubs.acs.org.

AUTHOR INFORMATION

Corresponding Author

*E-mail: olivier.mentre@ensc-lille.fr. Fax: (+) 33 3 20 43 68 14.

Notes

The authors declare no competing financial interest.

REFERENCES

(1) Burland, D. *Chem. Rev.* **1994**, *94*, 1.
(2) Min, K.; Ok, E.; Ok, Chi; Shiv Halasyamani, P. *Chem. Soc. Rev.* **2006**, *35*, 710−717.
(3) Pearson, R. G. *Proc. Natl. Acad. Sci. U.S.A.* **1975**, *72*, 2104−2106.
(4) Nguyen, S. D.; Yeon, J.; Kim, S.-H.; Halasyamani, P. S. *J. Am. Chem. Soc.* **2011**, *133*, 12422−12425.
(5) Yeon, J.; Kim, S.-H.; Hayward, M. A.; Halasyamani, P. S. *Inorg. Chem.* **2011**, *50*, 8663−8670.
(6) Izumi, H. K.; Kirsch, J. E.; Stern, C. L.; Poeppelmeier, K. R. *Inorg. Chem.* **2005**, *44*, 884−895.
(7) Charkin, D. O.; Kazakov, S. M.; Lebedev., D. N. *Russ. J. Inorg. Chem.* **2010**, *55*, 1248−1256.
(8) Huvé, M.; Colmont, M; Mentré, O. *Chem. Mater.* **2004**, *16*, 2628−2638.
(9) (a) Cornei, N.; Tancret, N.; Abraham, A.; Mentré, O. *Inorg. Chem.* **2006**, *45*, 4886−4888. (b) Krivovichev, S. V. *Solid State Sci.* **1999**, *1*, 211−219.
(10) Boivin, J. C.; Mairesse, G. *Chem. Mater.* **1998**, *10*, 2870−2888.
(11) Endara, D.; Colmont, M.; Huve, M.; Tricot, G.; Carpentier, L.; Mentre, O. *Inorg. Chem.* **2012**, DOI: 10.1021/ic201572y.
(12) Colmont, M.; Huvé, M.; Mentré, O. *Inorg. Chem.* **2006**, *45*, 6612−6621.
(13) Ketatni, E. M.; Mernari, B.; Abraham, F.; Mentré, O. *J. Solid State Chem.* **2000**, *153*, 48−54.
(14) Mentré, O.; Ketatni, E. M.; Colmont, M.; Huve, M.; Abraham, F.; Petricek, V. *J. Am. Chem. Soc.* **2006**, *128*, 10857−10867.
(15) Huvé, M.; Colmont, M.; Lejay, J.; Aschehoug, P.; Mentré, O. *Chem. Mater.* **2009**, 4019−4029.
(16) Huvé, M.; Colmont, M.; Mentré, O. *Inorg. Chem.* **2006**, *45*, 6604−6611.
(17) *SAINT+*, version 5.00; Bruker Analytical X-ray Systems: Madison, WI, 2001.
(18) *SADABS*, version 2.03; Bruker Analytical X-ray Systems: Madison, WI, 2001 (Bruker/Siemens Area detector absorption and other corrections).
(19) Petricek, V.; Dusek, M.; Palatinus, L. *JANA 2000*; Institut of Physics: Praha, Czech Republic, 2005.